EARTHQUAKE ENGINEERING AND STRUCTURAL DYNAMICS, VOL. 26, 859–874 (1997)

ANALYTICAL PREDICTION OF SEISMIC BEHAVIOUR FOR CONCENTRICALLY-BRACED STEEL SYSTEMS

ALEXANDER M. REMENNIKOV* AND WARREN R. WALPOLE
Department of Civil Engineering, University of Canterbury, Private Bag 4800, Christchurch, New Zealand

SUMMARY

This paper presents an analytical model for the inelastic response analysis of braced steel structures. A model is first presented for the behaviour of steel struts subjected to cyclic axial load, which combines the analytical formulation of plastic hinge behaviour with empirical formulas developed on the basis of experimental data. The brace is modelled as a pin-ended member, with a plastic hinge located at the midspan. Braces, with other end conditions, are handled using the effective length concept. Step-wise regression analysis is employed, to approximate the plastic conditions for the steel UC section. Verification of the brace model is performed on the basis of quasi-static analyses of individual struts and a one-bay one-storey X-braced steel frame. The comparison of analytical and experimental data has confirmed that the proposed brace model is able to accurately simulate the cyclic inelastic behaviour of steel braces and braced systems. A series of dynamic analyses has been performed on two-storey V- and X-braced frames to study the influence of brace slenderness ratio on the inelastic response, and to look at the redistribution of forces in the post-buckling range of behaviour of CBFs. Recommendations have been made as to the estimation of maximum storey drifts for concentrically-braced steel frames in major seismic event. © 1997 by John Wiley & Sons, Ltd.

Earthquake Engng. Struct. Dyn., **26**, 859–874 (1997)

No. of Figures: 10. No. of Tables: 0. No. of References: 28.

KEY WORDS: steel structures; braced frames; seismic behaviour; capacity design

1. INTRODUCTION

Structural steel is an ideal material for earthquake-resistant structural systems. It can exhibit such favourable, for seismic behaviour of structures, characteristics as material ductility and energy absorption. Investigation[1] of damage to structures in about 40 earthquakes has shown that buildings of structural steel have performed excellently and better than any other type of commercial and industrial structure in protecting life safety, limiting economic loss and business interruption.

However, considerable care is required in the design and detailing of steel frame systems and connections in order to make use of these favourable characteristics. The collapse of the 21-storey tower of the Piño Suarez complex, a high-rise, steel braced, moment-frame building, in the 1985 Mexico earthquake; and multiple failures of the beam–column connections of Moment-Resisting Frames (MRFs) in the 1994 Northridge earthquake, made it clear that much effort has yet to be made to ensure safe behaviour of the steel structures under severe earthquake attacks.

In New Zealand since the 1970s, a procedure of seismic design known as capacity design approach has been used, to ensure that the most appropriate mechanism of plastic deformation forms, in the event of

* Correspondence to: A. M. Remennikov, Department of Civil Engineering, University of Canterbury, Private Bag 4800, Christchurch, New Zealand. E-mail: remennam©cad.Canterbury.ac.nz.

Contract grant sponsor: NZ Foundation for Research, Science and Technology.

CCC 0098–8847/97/080859–16$17·50

Received 17 October 1996
Revised 16 January 1997

a severe earthquake. New Zealand Steel Structures Standard NZS 3404[2] presents detailed concepts and requirements when analysing and designing steel structures for earthquake resistance. According to NZS 3404, all steel seismic-resisting structural systems are classified into one of four categories for the purposes of seismic design: (1) Fully ductile systems (Category 1); (2) Systems of limited ductility capacity (Category 2); (3) Nominally elastic systems (Category 3A); and (4) Fully elastic systems (Category 3B). The provisions of the NZS 3404 are aimed at achieving non-brittle behaviour. Even fully elastic structural systems must not exhibit brittle modes of behaviour.

In NZS 3404[2], a Concentrically-Braced Frame (CBF) is defined as 'a braced frame in which the members are subjected primarily to axial forces'. CBFs with bracing effective in compression and tension may be either X-braced or V-braced. Such frames generally rely on inelastic deformations in the braces as the main source of earthquake energy dissipation. However, the cyclic inelastic behaviour of brace members is quite complex. In comparison with MRFs, braced frames may have limited reversible inelastic deformations.

For CBFs, similarly to MRFs, it would be desirable to enforce an inelastic mechanism, where the whole structure undergoes some inelastic deformation and plastic hinges spread over as many levels of the structure as possible, in order to reduce the magnitude of plastic deformations at particular locations. Once the braces at one level buckle or yield, then that level will tend to behave inelastically with the inherent tendency to form a soft storey. Computer simulations of dynamic behaviour of CBFs[3,4] have shown that inelastic deformations tend to concentrate in a few soft storeys near the bottom of the building.

It is thought that this tendency to form a soft storey mechanism may possibly be suppressed effectively if the capacity design procedure required in NZS 3404 is applied. According to this procedure for category 1, 2 CBF systems, the braces are chosen as the primary seismic-resisting elements, which produce the overstrength axial tension and compression actions. These overstrength brace actions are used then to design the beams, columns and connections. The columns are not permitted to be spliced at a storey level. So, the resulting strong, continuous column is supposed to act as passive suppressor against potential soft storey mechanism formation. The tentative capacity design procedures for all category 1, 2, and 3A CBF systems have already been outlined.[5] However, these procedures are based on a engineering assessment of CBF response, which is expected to be fairly conservative, and further analytical studies are needed to ensure the satisfactory performance of capacity-designed CBFs the severe seismic events. The present work is a part of a research programme, which aims at devising capacity design procedures for various types of CBFs.

2. CYCLIC RESPONSE OF STEEL BRACES

The cyclic behaviour of individual brace member has been studied both experimentally and analytically.[6–13] The results of these studies indicate a typical axial force–axial deformation relationship as shown in Figure 1(a).

The brace members are recognized to be a main source of earthquake energy dissipation in concentrically-braced steel frames. Such braced frames generally rely on inelastic deformations in braces, to absorb and

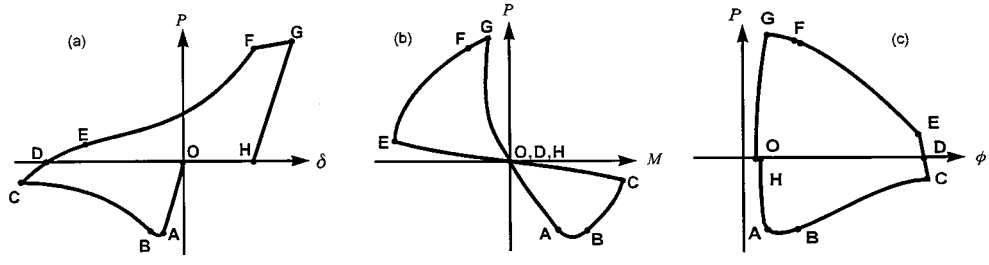

Figure 1. Definition of different zones: (a) P–δ curve; (b) P–M curve; (c) P–ϕ curve

dissipate earthquake energy demands. However, the hysteretic behaviour of bracing elements is quite complex. This cyclic behaviour involves such physical phenomena as the buckling of an element, the yielding of material, the local buckling effects, and the post-buckling deterioration of compressive load capacity, due to the Bauschinger effect and the tangent modulus deterioration.

The inelastic buckling of a brace, as a primary source of energy dissipation, results in the development of plastic hinges; that is, regions where inelastic curvatures take place. The number of plastic hinges that will form in a brace depends on the boundary conditions. Two idealized brace end conditions (both ends pinned and both ends fixed) are usually considered. The actual end restraint on braces in a real frame depends on a variety of factors such as, frame configuration, loading conditions, member slenderness ratio, joint flexibility, and inelastic behaviour of adjacent members. One plastic hinge forms in an idealized pinned-end brace and three hinges form in an idealized fixed-end brace.

For theoretical analysis, the general behaviour of the type shown in Figure 1 can be broken up into several zones. For a better representation of cyclic behaviour, following the zone definition of Ikeda,[12] a cycle is divided into four general categories: elastic zones, plastic zones, elastic buckling zone and the yield zone. The terms 'elastic' and 'plastic' correspond to the state of the plastic hinge, while the term 'yield' is associated with the state of the beam segments. After that, the elastic zone is subdivided into the elastic shortening (both member length and axial load decrease) and the elastic lengthening zone (both member length and axial load increase). Finally, the elastic shortening, the elastic lengthening and the plastic zones are further subdivided into the zones in compression and those in tension. As a result, the eight zones are incorporated to properly define axial force–deformation curve (see Figure 1(a)). The detailed description of each zone can be found elsewhere.[12,14]

The same zone definition also applies to the axial force–plastic hinge moment curve and to the axial force–plastic hinge rotation curve, as shown in Figure 1(a) and 1(b). Such detailed zone representation better reflects the distinctions of each zone, in particular, their irreversibility including 'elastic' zones. This irreversibility of 'elastic' zones arises mainly from the discontinuity of the tangent modulus at load history reversals.

3. TANGENT MODULUS HISTORY

The tangent modulus history, corresponding to the inelastic cyclic stretching and shortening of a column, is thought to be of a great importance for accurate prediction of the hysteretic behaviour for an individual brace. From the experimental results,[6,15] the tangent modulus of elasticity deteriorates significantly during inelastic reversals. Based on the test data, an empirical model was formulated[12] for the normalized tangent modulus $e = E_t/E$ as a function of the normalized axial force $p = P/P_y$ (see Figure 2). Two pairs of linear idealization curves are used to define the decrease and increase patterns. The values of four parameters e_1, e_2, e_3 and e_4 must be selected to account for available experimental data on the tangent modulus of elasticity. Originally,[12] the tangent modulus model was formulated for elastic-perfectly-plastic material behaviour. The model employed herein for developing an incremental brace model, is based on a work-hardening material model. The modifications to the original model have been made, so as to account for the degradation of these curves with cycles as observed in tests.

4. INCREMENTAL PHYSICAL THEORY BRACE MODEL

The physical model for a pin-ended brace member with a plastic hinge at midspan is shown in Figure 3. The member is loaded with an axial load P, that causes an internal plastic hinge moment M, the axial deformation δ and plastic hinge rotation Φ.

4.1. Yield surface function

The axial force–plastic hinge moment interaction relationship is used to define the fully plastic state in the centre hinge. States of force inside the interaction surface are assumed elastic; deformation hardening occurs

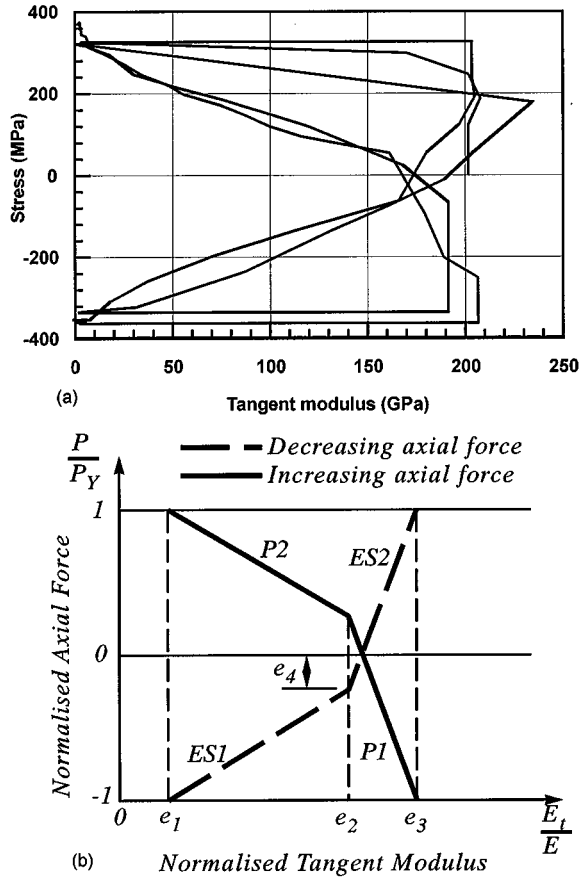

Figure 2. (a) Tangent modulus history; (b) tangent modulus empirical model

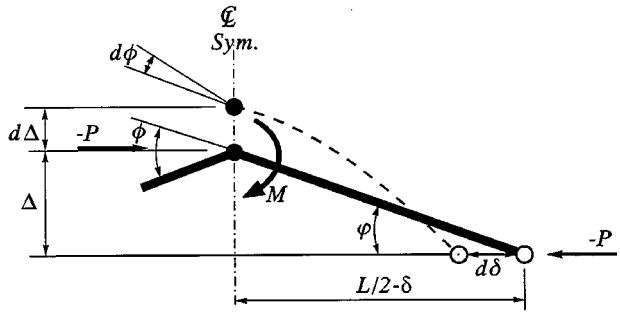

Figure 3. Deformed shape of a brace member

outside this surface. When the current yield surface is reached, the plastic flow rule[16] is used to define the orientation of the incremental plastic deformation vector.

An interaction curve for the initial yielding may serve as a yielding function for the cross section in the absence of residual stresses. A single and continuous function for structural steel was obtained by Orbison.[17]

The exact interaction curves for a 150UC30 section are depicted in Figure 4. A step-wise regression analysis was carried out making use of this analytical data. The modified yield surface function, which the best fits the exact solution data for a 150UC30 section, now takes the following form:

$$f = p^2 + m_x^2 + m_y^4 + 4{\cdot}05p^2m_x^2 + 8{\cdot}26p^6m_x^2 + 3{\cdot}68p^6m_y^2 + 10{\cdot}4p^6m_y^4 + 4{\cdot}65m_x^4m_y^2 - 1 = 0 \tag{1}$$

where $p = P/P_y$ is the normalized axial force; $m_x = M_x/M_{px}$ is the normalized strong axis bending moment; and $m_y = M_y/M_{py}$ is the normalized weak axis bending moment.

The comparison of the approximate and exact solutions is shown in Figure 4. It is seen that equation (1) is in good agreement with the plastification values. The correlation is particularly good for both the axial force–strong axis bending interaction and the axial force–weak axis bending interaction.

4.2. Basic equations

For simplicity, basic equations are developed for the right half of a brace member shown in Figure 3. The deflected shape of the brace can be obtained by solving the basic beam-column equation.[18] Then, the plastic hinge moment–plastic hinge rotation relationship can be established as

$$M = \gamma(v)\frac{E_tI}{L}\phi = \gamma(v)(E_tI)\Phi \tag{2}$$

where $\Phi = \phi/L$, and parameter $v^2 = |P|L^2/(E_tI)$. Hence, it follows that the plastic hinge rotation is expressed as

$$\Phi = (\gamma(v)E_tI)^{-1}M \tag{3}$$

where

$$\gamma(v) = \begin{cases} \dfrac{v}{2}\tan\dfrac{v}{2} & \text{if } P < 0 \\ -\dfrac{v}{2}\tanh\dfrac{v}{2} & \text{if } P > 0 \end{cases} \tag{4}$$

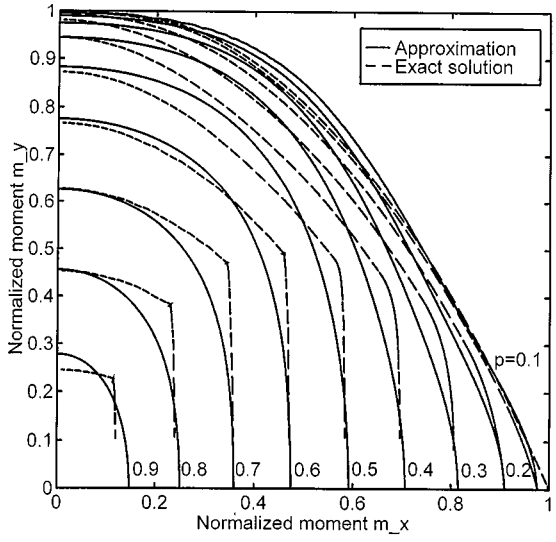

Figure 4. Biaxial interaction curves for 150UC30 section

The model formulation assumes elastic axial and flexural deformations along the length of the brace and plastic axial and flexural deformations concentrated in the plastic hinge. The total axial deformation increment, considering second-order effects, may be presented consisting of the following components:

$$\mathrm{d}\delta = \mathrm{d}\delta_{\mathrm{e}} + \mathrm{d}\delta_{\mathrm{g}} + \mathrm{d}\delta_{\mathrm{p}} + \mathrm{d}\delta_{\mathrm{ty}} \tag{5}$$

where δ_{e} is the elastic axial deformation; δ_{g} the geometric shortening deformation; δ_{p} the plastic hinge deformation; δ_{ty} the tensile yield deformation.

The elastic axial deformation increment, $\mathrm{d}\delta_{\mathrm{e}}$, is expressed as

$$\mathrm{d}\delta_{\mathrm{e}} = \{E_{\mathrm{t}}(P)A\}^{-1}\,\mathrm{d}P \tag{6}$$

where A is the cross-sectional area.

Geometric shortening deformation, δ_g, of a brace member may be expressed as follows:

$$\begin{aligned}\delta_{\mathrm{g}} &= -\frac{1}{2}\int_0^1 (\Delta'(x))^2\,\mathrm{d}x \\ &= -h_1(v)\phi^2 = -h_1(v)\Phi^2 L^2\end{aligned} \tag{7}$$

where

$$h_1(v) = \begin{cases} \dfrac{\sin v}{v} + 1 \\ \hline 16\cos^2\dfrac{v}{2} \end{cases} \quad \text{if } P < 0$$

$$h_1(v) = \begin{cases} \dfrac{\sinh v}{v} + 1 \\ \hline 16\cosh^2\dfrac{v}{2} \end{cases} \quad \text{if } P > 0 \tag{8}$$

Equation (7) can be introduced in an incremental form as follows:

$$\mathrm{d}\delta_{\mathrm{g}} = \langle S\rangle L^2\left[\frac{\mathrm{d}h_1(v)}{\mathrm{d}v}\frac{\mathrm{d}v}{\mathrm{d}P}\Phi_i^2 + 2h_1(v)\Phi_i\frac{\mathrm{d}\Phi(P_i)}{\mathrm{d}P}\right]\mathrm{d}P \tag{9}$$

in which subscript i denotes the values of forces P, moments M and rotation Φ before the change and

$$\langle S\rangle = \begin{cases} -1 & \text{if } P < 0 \\ +1 & \text{if } P > 0 \end{cases} \tag{10}$$

Incremental plastic deformation vector components, $\mathrm{d}\delta_{\mathrm{p}}$ and $\mathrm{d}\Phi_P$, can be evaluated on the basis of the plastic flow rule resulting from the Drucker's Postulate[16] and geometric considerations.[14] The following expressions for plastic deformation vector components have been derived:

$$\begin{aligned}\mathrm{d}\delta_{\mathrm{p}} &= \frac{f_{,P}(f_{,P}\,\mathrm{d}P + f_{,M}\,\mathrm{d}M)}{(E_{\mathrm{p}}A)f_{,P}^2 + (E_P I)f_{,M}^2}, \\ \mathrm{d}\Phi_{\mathrm{p}} &= \frac{f_{,M}(f_{,P}\,\mathrm{d}P + f_{,M}\,\mathrm{d}M)}{(E_{\mathrm{p}}A)f_{,P}^2 + (E_{\mathrm{p}}I)f_{,M}^2}\end{aligned} \tag{11}$$

where $f_{,P}$ and $f_{,M}$ are the derivatives of yield function f with respect to P and M, respectively, E_{p} the plastic modulus. Dividing the first line by the second line in equation (11), one can arrive at the following

expression for $d\delta_p$:

$$d\delta_p = \frac{f_{,P}}{f_{,M}} \frac{d\Phi_p}{dP} dP \tag{12}$$

The derivatives $f_{,P}$ and $f_{,M}$ can be easily calculated as soon as the explicit form of yielding surface or axial force–moment interaction curve is established. A method of evaluating the derivatives $dh_1(v)/dv$, dv/dP and $d\Phi/dP$ is given elsewhere.[14]

Finally, Equations (5), (6), (9) and (12) can be combined as

$$dP = K_t \, d\delta \tag{13}$$

where

$$K_t = \frac{E_t A}{1 + \langle S \rangle (E_t A) L^2 \left\{ \frac{dh_1(v)}{dv} \frac{dv}{dP} \Phi_i^2 + 2h_1(v) \Phi_i \frac{d\Phi_p}{dP} \right\} + (E_t A) \frac{f_{,P}}{f_{,M}} \frac{d\Phi_p}{dP}} \tag{14}$$

The tangent stiffness coefficient K_t defines the inelastic brace properties for an incremental solution. Equation (13) can be used to find the incremental axial force when the state is on the yield surface, and is loaded inelastically. From equation (11), the plastic hinge moment increment can be calculated as follows:

$$dM = \left[(E_p A) \frac{f_{,P}}{f_{,M}} + (E_p I) \frac{f_{,M}}{f_{,P}} \right] d\delta_p - \frac{f_{,P}}{f_{,M}} dP > 0 \tag{15}$$

in which an axial force increment, dP, is determined from equation (13); and a plastic deformation increment, $d\delta_p$, is defined by equation (12).

When the loading is elastic, $d\delta_p$ is equal to zero and equation (13) may be simplified as

$$dP = (E_t A) \left[1 + \langle S \rangle (E_t A) L^2 \left\{ \frac{dh_1(v)}{dv} \frac{dv}{dP} \Phi_i^2 + 2h_1(v) \Phi_i \frac{d\Phi_p}{dP} \right\} \right]^{-1} d\delta \tag{16}$$

This general equation can be used to get the incremental forces when the state is inside the yield surface, or when unloading from the yield surface.

From equations (6)–(16), stiffness and state determination algorithms for a computer model can be formulated. The incremental forces can be solved in terms of the incremental deformations by use of either equation (13) or (16).

In order to verify this model against experimental results, the data from the experiments by Leowardi[15] have been used to examine the cyclic buckling behaviour of braces. These authors reported test data for three struts tested under cyclic axial tension and compression loading. These three brace members and a stub column were made from a 150UC30 section supplied to AS3679-1990 Grade 250. Two of the struts are simply supported and the remaining one is fixed at both ends. Coupon tensile tests were carried out to determine values of yield stress and fracture strain. A stub column cyclic test was used to obtain cyclic stress–strain data, so that the tangent modulus history could be calculated.

The comparison of analytical and experimental data for two specimens with pinned–pinned and fixed–fixed boundary conditions is given herein. From the stub column cyclic test results,[14] the linear idealisation curves were suggested, so as to define the initial decrease pattern of tangent moduli of elasticity and, consequently, the parameters e_1, e_2, e_3, and e_4.

Several hardening rules of one-surface type[19] were employed to study the experimentally-observed phenomena in the cyclic behaviour of a brace member and to evaluate the effect on the analytical P–δ and P–M curves. Those hardening rules were implemented into the quasi-static computer program BRACE MODEL, and computer studies[14] made on the brace members demonstrated that the incremental physical theory brace model was able to represent cyclic buckling behaviour very well. Figure 5 shows the result of using the independent and mixed hardening rules for predicting the behaviour of specimens with different

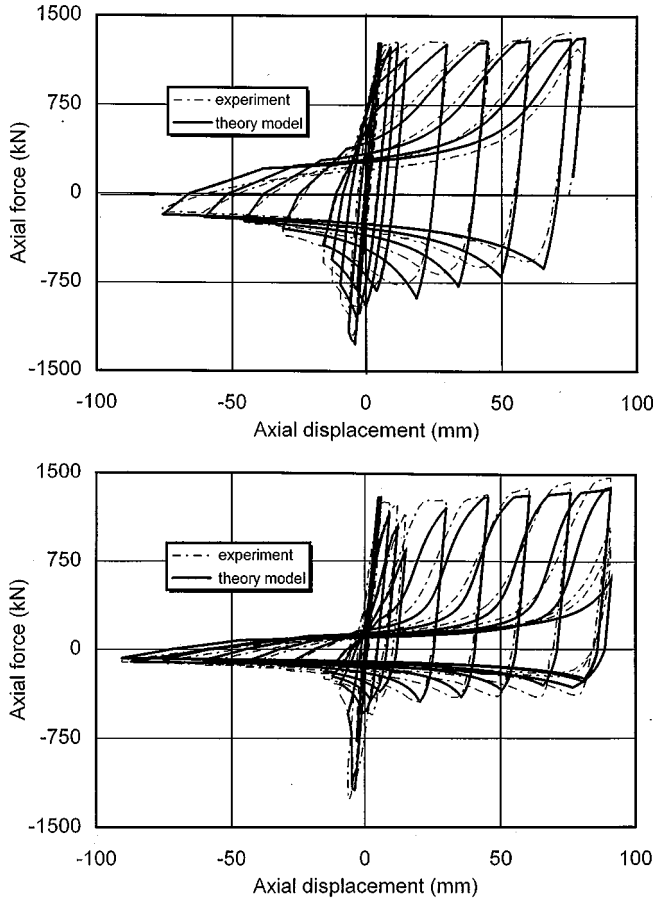

Figure 5. Comparison of analytical and experimental P–δ curves for fixed–fixed and pinned–pinned brace member

boundary conditions under cyclic loading. The presence of the phenomena mentioned above can be recognized. In both cases, the implemented hardening rules enabled the model to simulate the shifts of yield surface during later cycles in tension, the increase in the value of M_p in compression, as well as the deterioration in the buckling load with cycling.

The concept of effective member length was employed, while modelling the cyclic behaviour of the brace member with the fixed–fixed boundary conditions. Comparison of the results has confirmed that the analytical results for the fixed–fixed case are as good as those for the pinned–pinned case. One can expect that the proposed model can be used to analyse brace members with general boundary conditions. In addition, this model has been incorporated into the inelastic dynamic frame analysis program RUAUMOKO[20] to enable evaluation of the inelastic seismic response for steel braced structures.

5. SEISMIC BEHAVIOUR OF LOW-RISE BRACED FRAMES

Considerable analytical research has been performed on the modelling of the seismic behaviour of braced frames.[3,4,8,21] The physical theory brace models were employed in nearly all of these analyses. The study discussed hereinafter has been performed on the simple X- and V-braced frames shown in Figure 6 because of the limited experience with physical theory brace models in application to inelastic dynamic analyses.

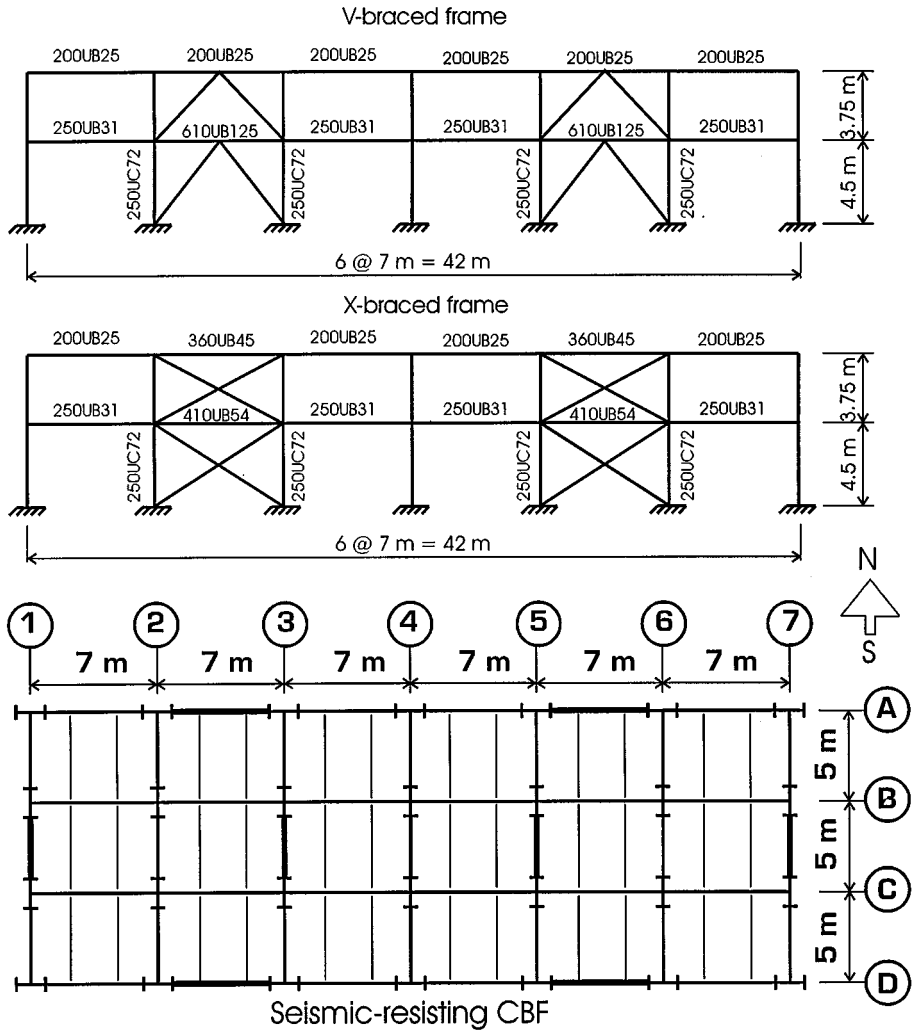

Figure 6. Floor plan and elevations of X- and V-braced frames

This study was aimed at the investigation of the inelastic force redistribution in braced steel frames, when subjected to seismic excitation. The objectives of the study, consequently, were, firstly, to estimate the maximum inelastic deflections and storey drifts that may develop in braced frames in a major earthquake; and secondly, to devise capacity design procedures for X- and V-braced frames to ensure their satisfactory inelastic performance under severe earthquake ground motions.

5.1. Building description and modelling

Two 2-storey buildings, one with chevron bracing and one with X-bracing, were designed according to the seismic design procedures for steel structures.[5] The selected structure is a six bays by three bays office building located in Wellington close to Wellington fault, one of the main expressions in central New Zealand of the boundary between the Pacific and Indian plates. The building height is 8·25 m, where the ground floor height is 4·5 m as shown in Figure 6. The framing system used is of a two-way braced type. The frames of the

two-way braced type are often used for their low unit cost and simple construction. The beam-to-column connections for such frames can be in the form of flexible end plates or web cleated connections. The seismic-resisting system for the structure in the E–W direction consists of the two perimeter six-bay CBFs along axes A and D. In the N–S direction, the seismic resisting system is four one-bay CBFs along axes 1, 3, 5 and 7. The frame selected for this study is a perimeter six-bay two-storey CBF along axis A, the elevation of which is shown in Figure 6. The frame is assumed to resist 50 per cent of the seismic loads in the E–W direction. The frame was designed for dead and live gravity loads. Floor construction was taken to consist of a beam and concrete slab floor system. Dead loads also included 1·2 kPa walls and partitions load. A live load of 2·5 kPa for the general office type of occupancy was taken according to NZS4203. The structure was designed to sustain seismic loads. The horizontal seismic shear force acting at the base of the structure in the direction being considered is given by formula $V = CW_t$, where the lateral force coefficient is defined by equation $C = C_h(T_1, \mu)S_pRZL_u$. The seismic hazard acceleration coefficient was selected from a set of design curves, that represent the constant ductility inelastic acceleration response spectra. Since the frame is designed as category 2 (limited ductility) CBF, the structural ductility factor was set as $\mu = 3$. The zone factor, Z, is equal to 0·4 for Wellington. The structural performance factor, S_p, is equal to 0·67 according to NZS4203. The risk factor, R, is equal to one and the limit state factor, L_u, is set as 1·0 for the ultimate limit state. The total seismic weight of building was calculated to be 6185 kN, while a half of the total weight was assigned to be a seismic weight of a seismic-resisting frame. The factor C_s needs to be determined before calculating the seismic base shear. The Steel Structures code NZS3404 specifies that the design seismic load for a category 1 or 2 CBFs is determined as a product of the lateral force coefficient C and the factor C_s, which is introduced to account for the less-than-ideal actual inelastic behaviour of X- and V-braced CBFs. For a two-storey braced frame with brace slenderness ratio from 80 to 120, the C_s factor is equal to 1·35. According to the selected parameters, the base shear was found to be 1295 kN, and fundamental period $T_1 = 0{\cdot}26$ sec.

The X- and V-braced frames were modelled using two types of one-dimensional elements incorporated in the RUAUMOKO computer program, namely, firstly, the Giberson One Component Beam element[20] which has a possible plastic hinge at one or both member ends; and, secondly, the Inelastic Steel Brace element discussed earlier. Tests[22,23] on X-braced frames showed that the deflected shape of a brace became unsymmetrical after several cycles of loading, because the bending deformation of the compression member under alternately repeated loading concentrated in one half. The other half gradually became straight as a number of loading cycles increased. It was noticed that the deflected shape of braces with large slenderness ratio became unsymmetrical more easily, than the ones with small slenderness ratio. Thus, only a half length of each bracing member was modelled making use of the inelastic brace model. This approach is justified by the experimental data for one-storey one-bay X-braced frame tested by Wakabayashi *et al.*[22] Figure 7(b) shows the simulated behaviour of the test frame[22] under repeated horizontal load, applied in a quasi-static way. Loading history was chosen to consist of displacement increments, rather than of load increments, because with buckling, a sudden force decrease will occur, and control over the frame behaviour will become difficult. One can see that the post-buckling behaviour of the compression bracing and the behaviour of the bent tension bracing results in the reversed S-shaped hysteretic loops. These loops can be compared with the experimental ones shown in Figure 7(a). Such a comparison reveals that the proposed approach for modelling X-braced frames gives correct trends and that the overall behaviour of the frame is in good conformity with the observations made during the experiment.

The columns and beams were represented by one-component beam elements. For dynamic analysis purposes, they were assumed massless and a lumped mass model was chosen, which assumes the mass of the structure is concentrated at the points at which the translational displacements are specified. The rotational mass of the nodal points was disregarded. The bolted connections between the beam and the column were assumed to be pinned. The connections between bracing members and frame were also idealized with pinned connection. An effective length factor, k_e, of 0·7 was employed for the X-bracings, whereas $k_e = 1{\cdot}0$ was used for V-bracings.

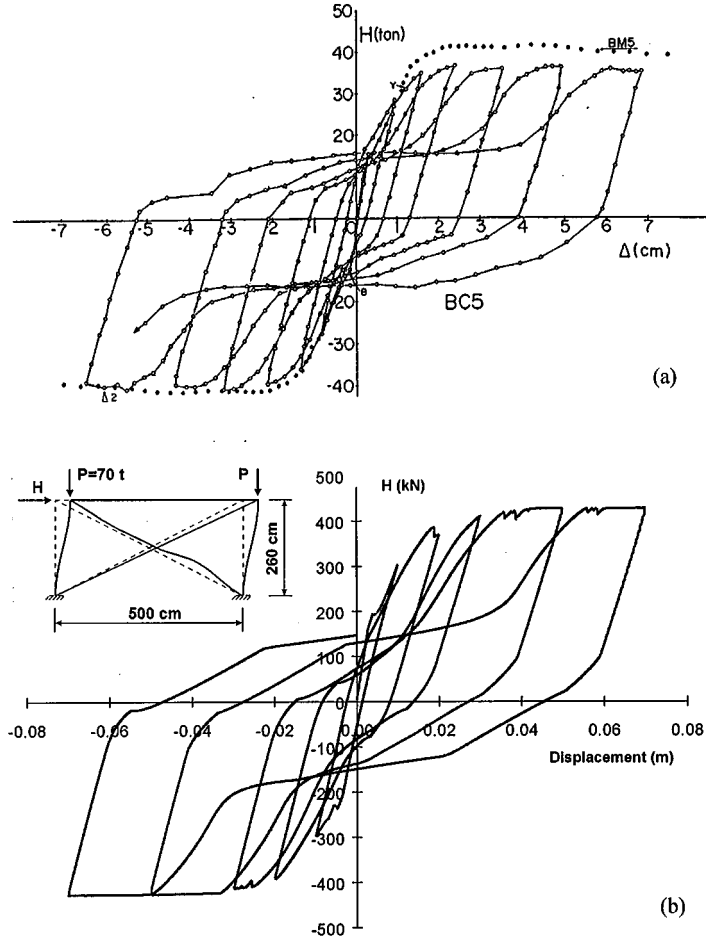

Figure 7. Behaviour of one-storey X-braced frame under repeated loading: (a) experimental (from Reference 24); (b) analytical prediction

The numerical time integration uses Newmark Constant Average Acceleration method, with a time step of 0·001 seconds to capture the important inelastic effects in a brace behaviour. Rayleigh-type damping conforming to 5 per cent in the first two modes was used. Three cycles of Newton–Raphson iteration is used at each time step to ensure convergence despite softening force–deformation characteristics.

5.2. Influence of brace slenderness on seismic performance of CBFs

The slenderness ratio of braces is considered to be the most important parameter, having a dominant influence on the seismic behaviour of braced frames. The provisions of NZS 3404, regarding the design of CBFs with bracing effective in tension and compression, are applicable only to CBFs containing bracing members with a slenderness ratio $k_e L/r$ not exceeding $120/\sqrt{(f_y/250)}$, where f_y is the yield stress used in design. According to the SEAOC (1990) recommendations, for structures above two storeys the ratio L/r (not $k_e L/r$) of braces is limited to a maximum value of $720/\sqrt{F_y}$ (= 120 for $F_y = 36$ ksi (250 MPa)).

NZS 3404 penalizes the CBFs for their 'less-than-ideal' behaviour under severe earthquake loading by applying the factor C_s ranging from 1·1 to 2·1 on top of the design seismic load determined in accordance

with the Loading Standards.[24] Despite the fact that this penalty is less severe for the CBFs with a compression brace slenderness ratio less than 40, the choice of a brace with a small $k_e L/r$ is not always ideal either. Such braces undergo severe plastic deformation in the post-buckling range. The curvatures associated with this cyclic inelastic bending may be very large and local buckling has to be expected. Such local buckling and the subsequent fracture have been observed rather early in tests on cold-formed RHS members.[5]

This section investigates the influence of the slenderness ratio $k_e L/r$ of brace members on the seismic performance of the CBFs. Values of 40 and 90 were chosen for the slenderness ratio. There is generally a limited range of rolled section sizes available and there are limits on what sections can be built-up. Usually, the designer will try to choose a member, which has a design resistance a little greater than the design load. The slenderness will be dependent on the cross-section chosen. For these reasons in this study, the buckling loads were kept constant for the members with different slenderness.

Seismic design provisions introduce a deflection amplification factor (DAF), to amplify the design drifts found from structural analysis, to estimate maximum storey drifts induced by major earthquakes. The design forces are obtained from the seismic forces, that would be induced if the frame remained elastic, by means of a Force Reduction Factor (FRF). The ratio of these factors DAF/FRF may be used to compare the responses of buildings. The DAF/FRF ratios for reinforced concrete moment frames used in several building codes were surveyed by Uang and Maarouf.[26] It has been shown that the DAF/FRF ratio can be determined as

$$\frac{\text{DAF}}{\text{FRF}} = \frac{\mu}{R_\mu} \tag{17}$$

where μ is the structure displacement ductility factor, defined as the ratio between the maximum inelastic displacement ($\Delta_{\max}$) and the displacement corresponding to the yield force (Δ_y); and R_μ is the ratio between the elastic force demand and the structure's idealized yield force level.

In present study, the maximum drift $\Delta_{\max}$ was obtained from a series of inelastic dynamic analyses. The 1940 N-S El-Centro earthquake record (PGA $= 0{\cdot}35g$) was utilized as the input ground motion for dynamic analyses. This is because the design acceleration response spectra presented by NZS 4203 are largely based on the response spectrum of the 1940 El-Centro earthquake record.

In this paper, the structure's idealized yield force level is defined, as the lowest intensity of the selected acceleration record, which causes buckling of the brace members. This was determined by scaling up or down the original earthquake record in accordance with the results of the elastic dynamic analysis and buckling characteristics of the most stressed braces used in the braced frames. Then, the earthquake record was scaled to several intensity levels in order to produce varying degree of inelastic response in the braced frames under consideration.

For each frame, each brace slenderness ratio and each intensity level of input ground motions the DAF/FRF ratios were computed. Figures 8(a) and 8(b) show the variations of the DAF/FRF ratios for estimating maximum storey drift as a function of the earthquake scaling factor R_μ. One can see that the DAF/FRF ratio increases with the force reduction factor and appears to be larger than one for both V- and X-braced frames except for the X-braced frame with stocky braces and a level of FRF up to 2·5.

The V-braced frame has demonstrated the poorest ability to sustain the inelastic demand, especially the frames with slender braces. Figure 8(a) shows that increase in brace slenderness ratio from 40 to 90, while maintaining the same level of brace compression strength, may result in the increased storey drift by a factor of two or more. It is also shown that for V-braced frames the ratio DAF/FRF varies from 3 to 5 even within the range of limited system ductility from 1 to 3 indicating considerable structural damage.

The X-braced frame has demonstrated much better ability to sustain the inelastic demands induced by earthquake load within the range of limited system ductility as shown in Figure 8(b). The DAF/FRF ratio appears to be 1·5–2·0 times higher for the frame with slender braces compared to the frame with stocky braces.

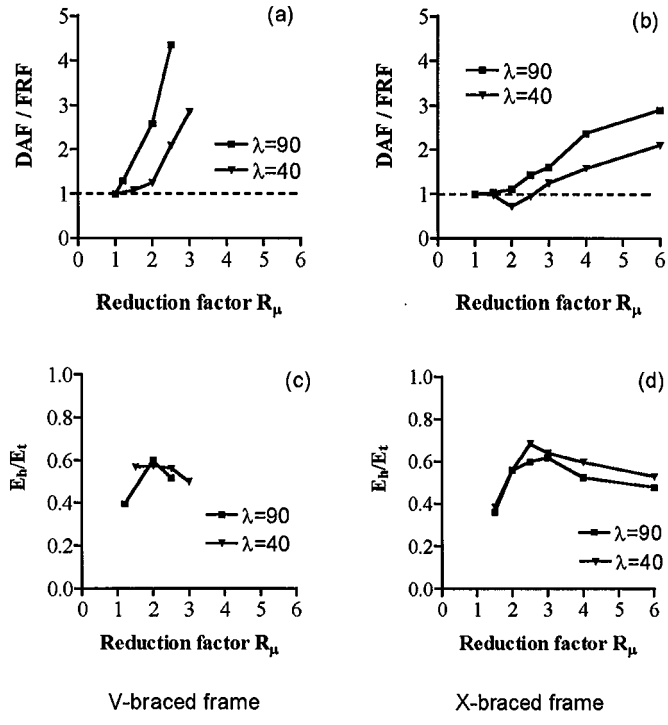

Figure 8. DAF/FRF and E_h/E_t ratios for V- and X-braced frames

In order to investigate the seismic energy dissipation characteristics of V- and X-braced frames, the ratios E_h/E_t, where E_h is the hysteretic energy absorbed by braces and E_t is the total input seismic energy, were estimated from the results of dynamic analyses. Figures 8(c) and 8(d) show the variation of the E_h/E_t ratios as a function of the earthquake scale factor R_μ. It appears that braces are capable of dissipating a significant amount (up to 60–70 per cent) of input seismic energy within the range of limited ductility demands on structure. The braced frames with stocky braces have demonstrated slightly better ability to dissipate seismic energy compared to the frames with slender braces with the same level of compression capacity. All cases studied have clearly demonstrated that there is a peak of seismic energy dissipation by braces which was around $R_\mu = 2{\cdot}5$–3, which suggests that the ratio of energy absorption to the total input energy has an upper limit. After that, the falling branch of the curves may indicate structural damage. Therefore, the peak of seismic energy disspation may indicate an acceptable value of the force reduction factor R_μ.

It appears that the incremental brace model was able to accurately predict the shape of the P–δ curves expected, for the slenderness ratios assumed. In fact, the braces were capable of dissipating seismic energy under cyclic loading. The braces with $k_e L/r$ of 40 demonstrated fuller hysteretic loops, and, as a result, the base shear–first-storey drift diagram shown in Figure 9 demonstrates minor nonlinearities in frame behaviour, within the range of limited system ductility demands. Figure 9 shows how the overall frame behaviour changes with increases in the values of $k_e L/r$ and R_μ. The hysteretic loops take on a severely pinched shape, and the structure's response becomes one-sided as a result of yielding and significant plastic deformation of one of the braces. The storey shear resistance of the bracing system is governed by the post-buckling behaviour of two crossed braces. The consequence will be a deteriorating base shear–storey drift relationship as that shown in Figure 9. One can see that the base shear–storey drift relationship exhibits more rapid deterioration with increase in a value of the $k_e L/r$.

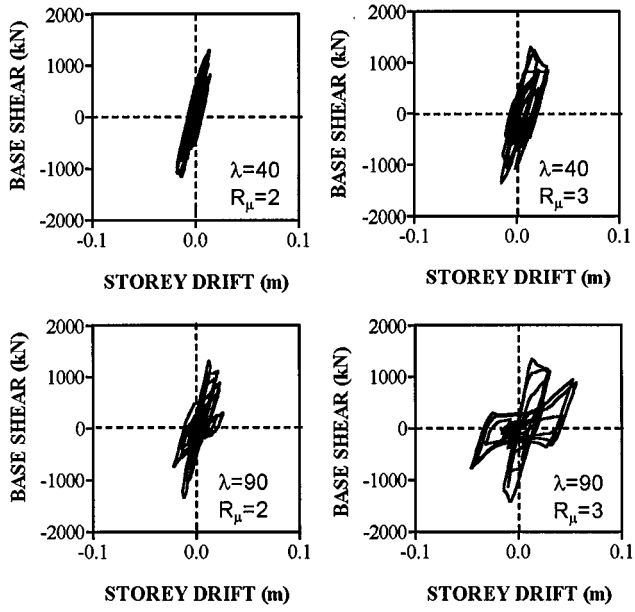

Figure 9. The base shear–first storey drift relationship for X-braced frame

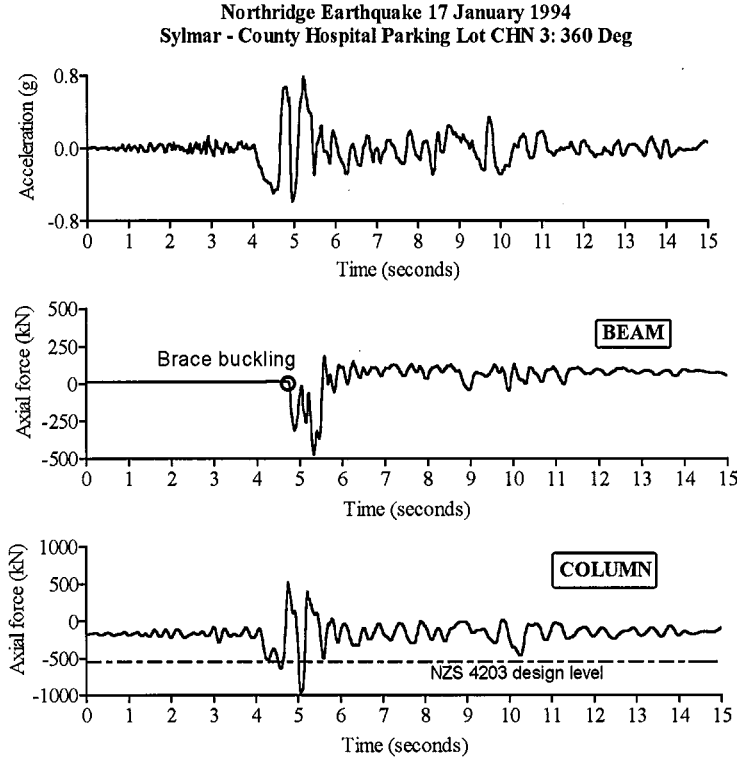

Figure 10. Time histories of axial forces in beam and column of seismic-resisting X-braced frame

5.3. Inelastic force redistribution and braced frames

Figure 10 shows the time-histories of seismic actions in beam and column elements of the V- and X-braced frames when subjected to the 1994 Northridge earthquake Sylmar County Hospital Parking Lot record (PGA = 0·82g). These demonstrate that inelastic force redistribution takes place in the braced frames, as a result of buckling of braces. The large axial forces in floor beams and columns are to be anticipated due to overstrength of the bracing. Such seismic force demands in the post-elastic range cannot be predicted by elastic structural analysis procedures and are not rationally accounted for in the current seismic code provisions. These issues are being now addressed by the authors in their on-going research programme on developing the capacity design methods for steel concentrically-braced frames under earthquake loading.

6. CONCLUSIONS AND RECOMMENDATIONS

This paper has highlighted some aspects of seismic behaviour and design implications for low-rise steel braced buildings. A brief overview of the cyclic inelastic response of steel bracing members has been presented. It appears, that an accurate prediction of the seismic behaviour of braced frames can be realized, with an accurate model of hysteretic behaviour for individual braces, with a wide range of slenderness ratios.

An incremental brace model for inelastic response analysis of CBFs, when subject to earthquake loading has been developed. The proposed model combines the analytical formulation of plastic hinge behaviour under the cyclic load, with empirical formulae based on a study of experimental data. The comparison of analytical and experimental results have demonstrated, that the incremental refined model is capable of simulating the overall cyclic behaviour of individual brace members.

A series of dynamic analyses has been performed on two-storey X- and V-braced steel frames which incorporated the inelastic brace elements. Parametric studies have been undertaken by varying the slenderness ratios of braces, while keeping the buckling capacities of braces constant. The following conclusions with regard to the studied inelastic performance of the braced frames can be drawn.

1. Based on analytically predicted inelastic seismic response of two steel braced building frames with X- and V-bracing configurations, the ductile behaviour of braced frames can be considered as being dependable only within the range of limited ductility demands, i.e. the structural ductility factor μ should not be greater than 3.
2. The deflection amplification factor used in NZS 4203 should be increased by a factor of two, when the maximum roof and storey drifts are of concern (e.g. when estimating the minimum seismic gap between buildings to avoid pounding). For frames with slender braces (λ = 80–120) a further increase in maximum interstorey drifts might be required.
3. More stringent regulations should be imposed on the use of V-braced frames, as the seismic-resisting system in high seismicity areas, even in low-rise buildings. Their design should be limited to the category 3A (nominally elastic systems with μ = 1·25) and to the use of braces with low slenderness ratios.

It has also been shown, that the post-buckling force redistribution takes place in the braced frames, but it is not very sensitive to brace slenderness ratios (while maintaining the constant buckling strength). This force redistribution cannot be predicted by the equivalent static nor the modal response spectrum methods (e.g., large axial force in the beam) and can be underestimated (e.g., increased column compression after brace buckling). The results obtained in this investigation confirm, the necessity for developing the design methods for steel CBFs, which are based on a 'capacity design' philosophy,[2,7] widely accepted for reinforced concrete structures. The interim provisions for capacity design of CBFs have already been formulated.[5] The work on a detailed analysis and verification of these procedures is in progress now at the Department of Civil Engineering, University of Canterbury.

ACKNOWLEDGMENTS

This research has been carried out under the grant of the NZ Foundation for Research, Science and Technology for the first author. The authors wish to thank Dr Athol Carr for his constant interest in this work and for his help with the RUAUMOKO computer program.

REFERENCES

1. P. I. Yanev and J. D. Gillengerten, 'The performance of steel structures in past earthquakes', *Proc. nat. steel construction conf.*, Washington, 1991.
2. *NZS 3404. Steel Structures Standard*. New Zealand, 1992.
3. I. F. Khatib, S. A. Mahin and K. S. Pister, 'Seismic behaviour of concentrically braced steel frames', *Report UCB/EERC 88/01*, Earthquake Engineering Research Centre, University of Berkeley CA, 1988.
4. F. Perotti and G. P. Scarlassara, 'Concentrically braced steel frames under seismic actions: non-linear behaviour and design coefficients', *Earthquake Engng. Struct. Dyn.* **20**, 409–427 (1991).
5. New Zealand Heavy Engineering Research Association, *Seismic Design Procedures for Steel Structures*, *HERA Report 74-6*, Manukau City, New Zealand, 1995.
6. R. G. Black, W. Wenger and E. P. Popov, 'Inelastic buckling of steel strut under cyclic load reversals', *EERC Report No. 80/40*, Earthquake Engineering Research Center, University of California at Berkeley, CA, 1980.
7. A. K. Jain and S. C. Goel, 'Hysteresis models for steel members subjected to cyclic buckling or cyclic end moments and buckling', *UMEE Report No. 78R6*, University of Michigan at Ann Arbor, 1978.
8. X. Tang and S. C. Goel, 'Seismic analysis and design considerations of braced steel structures', *UMCE Report No. 87-4*, University of Michigan at Ann Arbor, 1987.
9. B. Maison and E. P. Popov, 'Cyclic response prediction for braced steel frames', *J. struct. div. ASCE*, **106**(ST7), 1401–1416 (1980).
10. T. Nonaka, 'An elastic–plastic analysis of a bar under repeated axial loading', *Int. j. solids struct.* **9**, 569–580 (1973).
11. .H. Gugerli and S. C. Goel, 'Inelastic cyclic behaviour of steel bracing members', *UMEE Report No. 82R1*, Department of Civil Engineering, University of Michigan at Ann Arbor, 1982.
12. K. Ikeda and S. A. Mahin, 'A refined physical theory model for predicting the seismic behavior of braced steel frames', *EERC Report No. 84/12*, Earthquake Engineering Research Center, University of California at Berkeley, CA, 1984.
13. G. Ballio and F. Perotti, 'Cyclic behaviour of axially loaded members; numerical simulation and experimental verification', *J. construct. steel res.* **7**, 3–41 (1987).
14. A. M. Remennikov and W. R. Walpole, 'Incremental model for predicting the inelastic hysteretic behaviour of steel bracing members', *Research Report 95-6*, Department of Civil Engineering, University of Canterbury, Christchurch, New Zealand.
15. L. S. Leowardi, 'Performance of steel brace members', *ME Thesis*, University of Canterbury, Christchurch, New Zealand, 1994.
16. D. C. Drucker, *Plasticity*, *Structural Mechanics*, Pergamon Press, London, 1960, pp. 407–488.
17. J. G. Orbison, W. McGuire and J. F. Abel, 'Yield surface applications in non-linear steel frame analysis', *Comput. methods appl. mech. eng.*, **33**(1–3), 557–573 (1982).
18. W. F. Chen and T. Atsuta, *Theory of Beam-Columns*, Vol. 2, McGraw-Hill, New York, 1977.
19. W. F. Chen and D. J. Han, *Plasticity for structural engineers*, Springer, New York, 1988.
20. A. J. Carr, '*RUAUMOKO*', Computer Program Library, Department of Civil Engineering, University of Canterbury, New Zealand.
21. F. Perotti, A. De Amici and P. Venturini, 'Numerical analysis and design implications of the seismic behaviour of one-storey steel bracing systems', *Eng. struct.* **18**, 162–178 (1996).
22. M. Wakabayashi *et al.*, 'Inelastic behaviour of full-scale steel frames with and without bracings', *Bull. disas. prev. res. inst.*, Kyoto Univ. **24**, Part 1 (216), 1–23 (1974).
23. M. Wakabayashi *et al.*, 'Experimental studies on the elastic-plastic behaviour of braced frames under repeated horizontal loading', *Bull. disas. prev. res. inst.*, Kyoto Univ. **27**, Part 3 (251), 121–154 (1977).
24. *NZS 4203. General Structural Design and Design Loadings for Buildings*, New Zealand, 1992.
25. W. R. Walpole, 'Behaviour of cold-formed steel RHS members under cyclic loading', *Proc. NZNSEE conf.*, *Wairakei*, New Zealand, 1994.
26. C.-M. Uang and A. Maarouf, 'Estimating seismic drifts of multistory reinforced concrete frames', *Struct. Design Tall Build.* **4**, 61–70 (1995).
27. T. Paulay and M. J. N. Priestley, *Seismic Design of Reinforced Concrete and Masonry Buildings*, Wiley, New York, 1992.
28. N. S. Trahair and M. A. Bradford, *The Behaviour and Design of Steel Structures*, Chapman and Hall, London, 1991.

